PERGAMON

Building and Environment 35 (2000) 633–644

BUILDING AND ENVIRONMENT

www.elsevier.com/locate/buildenv

# TRNSHD — a program for shading and insolation calculations

Marion D.E. Hiller, William A. Beckman, John W. Mitchell*

*University of Wisconsin-Madison, Solar Energy Laboratory, Department of Mechanical Engineering, 1513 University Avenue, Madison, WI 53706-1572, USA*

Received 7 July 1998; received in revised form 17 May 1999; accepted 24 August 1999

**Abstract**

For analyzing systems with high solar gains it is important that design tools have a reliable and accurate means of predicting the solar radiation on surfaces. Since solar radiation on a surface is often greatly influenced by self-associated facade obstructions, neighbor buildings and the surrounding landscape, a prerequisite of solar modeling is the ability to predict shaded and unshaded building parts as a function of solar position and geometry.

This paper introduces a new simulation program called TRNSHD for external shading and internal insolation calculations of buildings. Although TRNSHD was developed for building simulations with TRNSYS, it is a stand-alone tool that is not restricted to either buildings or TRNSYS and thus can be used to solve other shading problems. The program can handle a large variety of surface shapes as well as beam and diffuse radiation. TRNSHD calculations were compared with other algorithms, measurements and proposed European Standard. The validation shows that TRNSHD functions correctly and that the results of TRNSHD are in good agreement with expected values. A complex shading case study of a building with an atrium has been performed by using TRNSHD. The study gives an example of the use of the program and demonstrates its capabilities. 

## 1. Introduction

The energy consumption of US buildings accounts for 36% of the country's energy supply at a cost of \$193 billion and the energy use is growing at a rate of 3.3% a year. Heating and cooling equipment consumes 42% of all building energy use at a cost of \$81 billion. Buildings that incorporate a passive solar design can save as much as 50% on heating bills for only 1% more construction cost [1].

These facts illustrate the capability and the importance of passive solar building design with respect to conservation of both energy and money. But applying passive solar effectively requires information and attention to the details of design and construction. Nowadays, design tools are available to analyze the thermal behavior of buildings in detail and give recommendations for design strategies. It is therefore necessary that design tools have a reliable and accurate means of predicting the solar radiation on surfaces.

Due to its intensive development in the last years, the simulation program TRNSYS has become an attractive tool for the thermal analysis of buildings. A new graphical interface called TRNSCAD offers a convenient way to describe the building geometry in three dimensions. This new input feature provides the complete three dimensional geometric information so that advanced methods can be incorporated for calculating the external shading and inside insolation on surfaces.

The standard shading model of TRNSYS, TYPE 34 (overhang and wingwall shading), is restricted to a special geometrical configuration of surfaces and the large effort needed to specify the geometric information is inconvenient, especially when many surfaces might be shaded. Due to this restriction, the shading of tilted surfaces cannot be determined. Also, shadows from opposite or tilted surfaces, building parts and the

* Corresponding author. Tel.: +1-608-262-5972; fax: +1-608-262-8464.

*E-mail address:* mitchell@engr.wisc.edu (J.W. Mitchell).

0360-1323/00/\$ - see front matter 
PII: S0360-1323(99)00051-7

surrounding landscape cannot be represented. For calculating the insolation on inside surfaces, TYPE 56 uses constant absorptance weighted area ratios. This simple method works fine, if all internal walls are opaque. However, when internal windows are also considered, the penetration of direct solar radiation from one building zone to another causes modeling problems. The capability of modeling such effects is especially important for buildings with high solar gains and internal glazing, like sunspaces and atria.

Therefore, a new program called TRNSHD has been developed to offer a more comprehensive and general method of external surface shading and internal solar distribution calculations for building simulations.

## 2. Program description

### 2.1. Input data

The program TRNSHD requires as input a data file containing the geometric information of the building and its obstructions. This geometric information must satisfy the data structure as shown in Fig. 1. The building is composed of modules, which are three-dimensional convex polyhedral solids. The modules can be disjoint or touching each other at a common vertex, edge or face, but modules are not allowed to penetrate one another. Obstructions are considered as two-dimensional planar polygons with a zero transparency. All walls, windows and obstructions are considered as planar non-selfintersecting polygons without holes. The edges of a polygon are restricted to straight lines. The boundary of the polygon is represented by an ordered circular list of its vertices. The building and its obstructions are defined in a coordinate system, the so-called world coordinate system.

In addition to the geometric input, TRNSHD allows the user to select the desired calculation level in an interactive way. With regard to the computation time, the lowest acceptable level of detail should be selected. The following calculation modes are available:

- beam radiation shading calculation of external surfaces ON/OFF and;
- diffuse radiation shading calculations of external surfaces ON/OFF and;
- internal insolation distribution of beam radiation ON/OFF.

If the calculation of beam radiation shading is turned on, then TRNSHD needs information about the location of the building in order to determine the sun's position correctly:

- latitude of the location in question;
- a switch to indicate that the program should per-

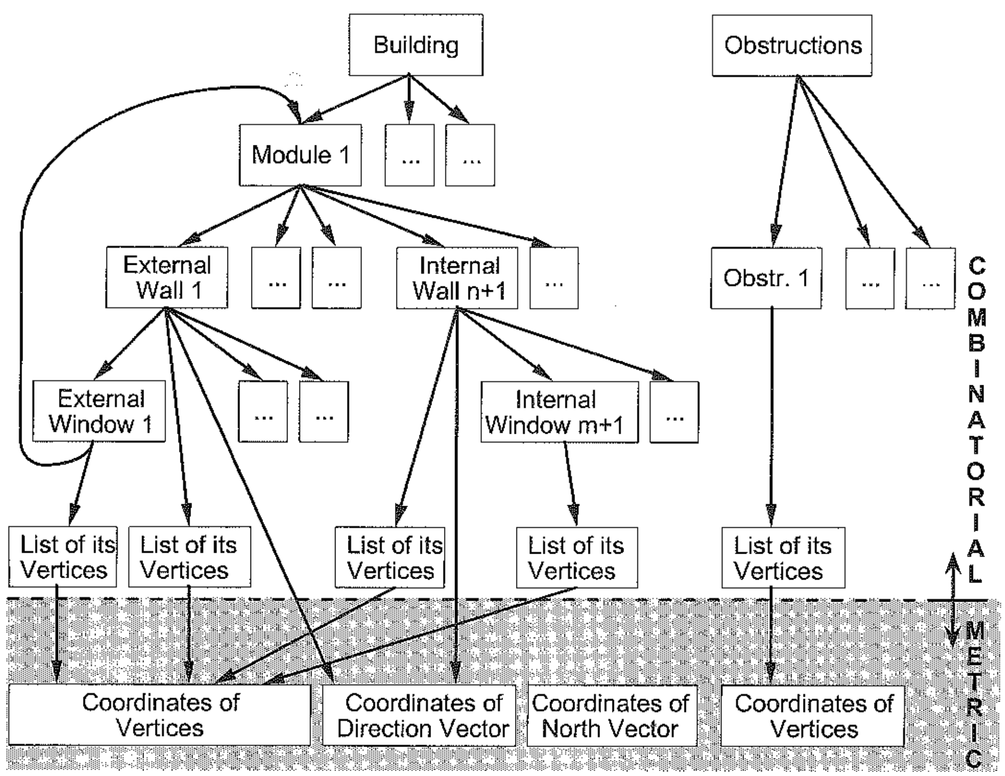


Fig. 1. Data structure of the geometric input.

form the calculations in solar time or;

- the difference between the standard meridian for the local time zone and the longitude of the location in question (called SHFT).

### 2.2. Beam radiation modeling

The solar position is determined for each hour of one day of each month. The chosen day corresponds to the average day of that month according to Klein [2]. For each hour the average solar position is used. The restriction to one day a month is a common approach used for shading calculations of building and is a reasonable compromise between accuracy and computing effort. The effects on the calculation results by using an average day instead of accurate daily calculations are discussed by Hiller [13]. Shading calculations for a south-facing window with an overhang and two wingwalls were carried out each day for one month on an hourly basis. The chosen month corresponds to the month of the year with the largest deviation of the declination throughout the month. The discussion by Hiller [13] yields to the conclusion that using an average day is a good choice and more accurate than using the first day of a month. The position of the sun in the sky is specified by two solar angles, the solar zenith angle and the solar azimuth angle. The zenith angle is the angle between the vertical and the line to the sun. The solar azimuth angle is the angle between the local meridian and the projection of the line of sight of the sun onto the horizontal plane. For determining both solar angles TYPE 16 (solar radiation processor) of TRNSYS [3] was modified and implemented as a subroutine. The coordinates of the sun direction vector in the world coordinate are obtained from the solar angles and the angle $\alpha_N$ between the $x$-axis of the worlds coordinate system and the given north vector.

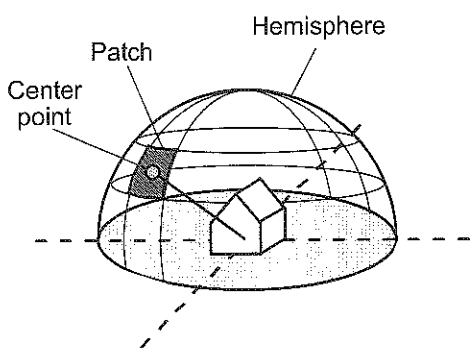


Fig. 2. Discretization for diffuse radiation calculations.

### 2.3. Diffuse radiation modeling

For modeling (short-wave) diffuse sky radiation, an approach implemented in DOE-2 [4] is adopted. The method basically subdivides the diffuse radiation problem into several "beam" radiation problems. The sky is represented by a half hemisphere, where the building is placed in its center (see Fig. 2). This half hemisphere is subdivided into 12 × 6 patches. The increment angle for the azimuth angle is set to 30° and the increment angle of the zenith angle to 15°. It is assumed that the patches are rather small and far away, thus the diffuse radiation leaving each patch can be treated as parallel radiation with the direction from its center point to the center of the hemisphere. Similar to the sun's position for beam radiation, a "sun's position" for diffuse radiation can then be defined as the center point of a patch and described by the same two solar angles, the solar zenith and azimuth angle. A routine creates the center points of all patches by defining the solar zenith and azimuth angle and then calculates the diffuse sun vectors.

### 2.4. Geometric calculations

The program selects each external wall of the building in turn as the wall receiving radiation for the shading calculations. The shading calculations begin with a coordinate transformation of all vertices to a more convenient coordinate system, the wall coordinate system, where the positive $x$-axis is equal to the direction of the outward drawn normal vector of the current receiving wall. Due to the coordinate transformation the pretesting and projection of shadow casting surfaces are easier to perform. Then, a preliminary test called "quadrant test" is performed. The quadrant test eliminates all potential shadow casting surfaces, which lie completely behind the current receiving wall. TRNSHD considers all external walls and obstructions automatically as potential shadow casting surfaces. Potential shadow casting surfaces that lie partially behind the receiving wall are detected and marked for special treatment during the projection procedure. This step is necessary in order to avoid false shadow projection. The remaining surfaces are presorted and classified into four groups. Each group corresponds to a "sun quadrant" which is the quadrant of the wall coordinate system where the sun is currently located. Due to the subdivision of the shadow casting surfaces into four groups, the number of potential shadow casting surfaces for a specific sun position can be greatly reduced. The results of the quadrant test make it easy to decide at an early stage whether the receiving wall can actually be shaded or not. After the Quadrant Test, the program sets up loops over all solar positions. Within the loop, the program checks first, whether the current receiving wall is sunlit or not. Afterwards, the three-dimensional problem is reduced to two dimensions by projecting potential shadow casting surfaces onto the plane of the current receiving wall according to the sun's ray. In the projection procedure, only the shaded external walls are projected, because it is not necessary to project both sunlit and shaded surfaces of a polyhedral solid [5]. It is more convenient to consider the shaded surfaces of a building, because in general there are less shaded surfaces remaining after quadrant test than sunlit surfaces. After the projection, the program eliminates shadow casting surfaces, which lie completely below, above, right and left with respect to the receiving surface, respectively. Many cases in which no shadow is cast on the receiving wall will be eliminated through this step. A clipping procedure determines then the boundary of the sunlit parts of the current receiving wall according to a vector based method proposed by [6]. The method is described later in detail. After the clipping procedure, the sunlit fraction of beam radiation is determined by:

$$f_{\text{beam, ex}} = \frac{A_{\text{sunlit}}}{A_{\text{total}}} \tag{1}$$

where $A_{\text{sunlit}}$ is the sunlit area of the receiving surface and $A_{\text{total}}$ is the total area of the receiving surface.

The area of the sunlit parts as well as the whole surface is calculated by [7]:

$$A = \frac{1}{2}\sum_{k=1}^{n}(Y_k Z_{k-1} - Y_{k-1} Z_k) \tag{2}$$

where $Y_k$, $Z_k$ are coordinates of the vertex $k$, and $Y_1 = Y_n$, $Z_1 = Z_n$ and $n$ is the number of vertices of the surface.

After the wall clipping, the program selects each attached window of the wall in turn, performs the clipping process and determines the sunlit fractions. If the internal solar distribution is turned on, then TRNSHD computes the sunlit fractions of the window that strike each internal surface of the module. The performed calculation steps are similar to the external surface shading. All sunlit inside surfaces are projected onto the plane of the window and clipped against the remaining (sunlit) parts of the window obtained from the external shading calculations. After each clipping process the remaining sunlit area of the receiving window is calculated and therewith the sunlit fraction of the inside wall and window, respectively:

$$f_{\text{beam, in}} = \frac{A_{\text{sunlit, total}} - A_{\text{sunlit, after}}}{A_{\text{sunlit, total}}} \tag{3}$$

where $A_{\text{sunlit,after}}$ is the sunlit area of the receiving window after the clipping process and $A_{\text{sunlit,total}}$ is the sunlit area of the receiving window after the external shading calculations.

After finishing the attached window loop, the sunlit fractions of the receiving wall and its attached windows are computed for diffuse radiation. The diffuse fraction $f_{\text{dfu,ex}}$ of an external surfaces is determined by the following equations:

$$f_{\text{dfu, ex}} = \frac{\sum_{k=1}^{n} \cos\ \alpha_k \Delta\omega_k f_{\text{beam, }k}}{\sum_{k=1}^{n} \cos\ \alpha_k \Delta\omega_k} \tag{4}$$

$$\Delta\omega_k = \sin\theta_{Z,\ k}\Delta\theta_Z \Delta\omega_Z \Delta\gamma \tag{5}$$

where $n$ is the number of patches where receiving surface is sunlit, $\alpha_k$ is the angle between the surface normal vector and the sun vector of patch $k$, $\theta_{Z,k}$ is the solar zenith angle of patch $k$, $f_{\text{beam},k}$ is the "beam" sunlit fraction of patch $k$, $\Delta\omega_{Z,}$ is the increment of the solid angle of patch $k$, $\Delta\gamma$ is the increment of the solar azimuth angle of patch, $\Delta\theta_{Z,}$ is the increment of the solar zenith angle of patch.

All calculated sunlit fractions are written to output files and the program continues with the next external wall as receiving wall. The program terminates after the shading calculations have been performed for each external wall.

### 2.5. Polygon clipping

The clipping procedure is based on an approach by [6]. The procedure itself is performed by a subroutine based on a MS thesis of Johnston [8] at the University of Wisconsin–Milwaukee. Fundamental improvements in Johnston's program, especially at the intersection part, were made in order to obtain correct results. The receiving and shadow casting surfaces are presented as polygons by an ordered circular list of their vertices. In order to determine the sunlit parts of the receiving polygon and the shadow casting polygons, the receiving polygon is ordered counter clockwise and the shadow casting polygons clockwise. The actual order of a polygon can be determined by the sign of its area calculated according to Eq. (2). If the area is negative, the vertices are ordered counter clockwise; otherwise they are ordered clockwise. The procedure consists of two main parts:

- intersection testing; and
- boundary evaluation.

The first step in the algorithm is to determine the intersecting points of both polygons. The intersections are classified into entering intersections, where the shadow casting polygon enters the receiving polygon, and leaving intersections, where the shadow casting polygon leaves the receiving polygon. Entering and leaving intersections must occur in pairs. If none of the intersections is a vertex of one of the polygons, the classification of the first intersection, and thus of all other intersections, is obtained by a point membership test of first vertex of the shadow casting polygon with respect to the receiving polygon. However, if intersections are vertices of one of the two polygons, neighbor point tests must be performed in order to determine their correct classification. After the intersection classification, a second list of the intersections is established. Whereas the first list holds the intersections in the order they occur on the shadow casting polygon, the second list holds the intersections in the order they occur on the receiving polygon.

If more than one intersection is detected, a boundary traversal is performed in order to obtain the non-overlapping parts of the receiving polygon. The basic boundary traversal, as shown in Fig. 3, starts at the first entering intersection on the shadow casting polygon and follows its boundary until the next intersection is found. At the second intersection the algorithm switches to the receiving polygon and follows the boundary of the receiving polygon until the next intersection is found. Again the algorithm switches, this time to the shadow casting polygon and the boundary of the shadow casting polygon is then followed. The boundary traversal is continued until the starting point is reached as shown in Fig. 3. The clipping process is not finished until all intersections have been stored during the boundary traversal. If some intersections have not been stored, then more than one remaining sunlit polygon exists and a new boundary traversal starts at the first unstored intersection on the shadow casting polygon.

If one or zero intersections are encountered, both polygons are either disjoint (no intersection) or touching each other (one intersection). This means that the receiving polygon might be completely shaded, completely unshaded or possess an inscribed shader. In order to distinguish those cases, a point membership classification of a boundary point of the shadow casting polygon with respect to the receiving polygon and visa versa are performed. If both points are found to be outside, the polygons are disjoint and no shading occurs. If the boundary point of the receiving polygon is found to be inside the shadow casting polygon, but the boundary point of the shadow casting polygon is outside, then the receiving polygon lies inside the shadow casting polygon and is completely shaded. The remaining case is an inscribed shadow casting polygon. In order to avoid polygons with holes, the remaining receiving polygon is subdivided into two simple connected polygons.

This quite complex, but powerful clipping method allows an accurate determination of the non-overlapping parts of planar polygons in two dimensions. It is able to handle all kinds of polygons. Another advantage of this method is that the remaining sunlit or shaded polygons are represented the same way as the original receiving polygon. Therefore, the output polygons can be directly used for further calculations like the internal distribution of beam radiation. The Weiler–Atherton method can also be extended to semi-transparent shadow casting surfaces. Therefore, not only the non-overlapping parts, but also the overlapping parts with semi-transparent shadow casting polygons must determined. This can be done by performing the above described boundary traversal with a clockwise ordered receiving polygon.

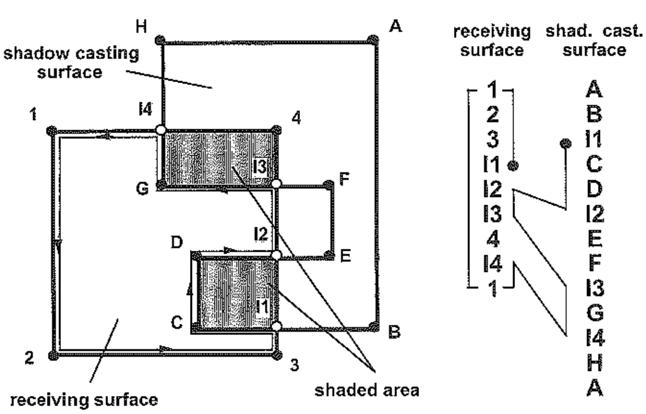


Fig. 3. Boundary evaluation by polygon clipping.

## 3. Validation

For validation, the results of TRNSHD are compared with other algorithms, measurements and a proposed European Standard (CEN). Each calculation mode is validated separately. In addition, the major assumptions of TRNSHD and their effects on the results are discussed.

## 4. Beam radiation shading

### *4.1. Validation against TRNSYS TYPE 34 (ASHRAE standard algorithm)*

Up to now, the blocking of solar radiation in TRNSYS has been performed by TYPE 34, overhang and wingwall shading. TYPE 34 calculates the shading of beam, diffuse and ground reflected radiation of a vertical rectangular receiver surface due to rectangular overhang and wingwalls.

For comparison, shading calculations of beam radiation for simple geometric configurations were carried

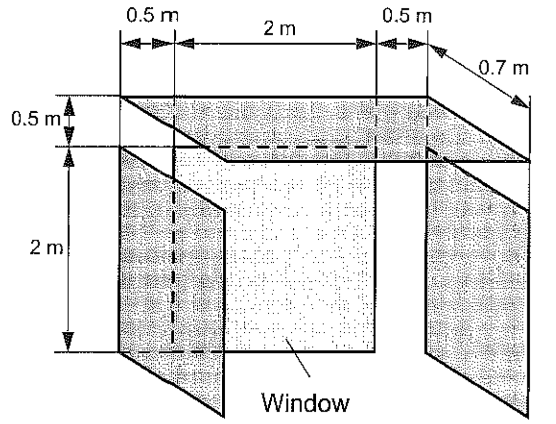


Fig. 4. Dimensions of the shading configuration.

out with both programs TYPE 34 with TRNSYS and TRNSHD. Both programs use the same algorithm to calculate the solar position, but the algorithms that determine the sunlit area are different. TYPE 34 uses an ASHRAE algorithm [9] that was contributed by Sun, whereas TRNSHD employs the Weiler–Atherton method (see Section 2). The dimensions of the example receiving surface and its obstructions are shown in Fig. 4. The receiving surface is a vertical south-facing window located in Madison, WI at a latitude of 43.1° N and a longitude of 89.4°. The window can be shaded by up to two wingwalls and an overhang. The shading calculations were performed on 17 July in local time. The resulting sunlit fractions for four shading configurations are shown in Fig. 5. The results of both programs show good agreement, they give the same results to five significant digits.

### 4.2. Validation against a proposed European Standard (CEN)

The proposed European Standard [10] specifies the

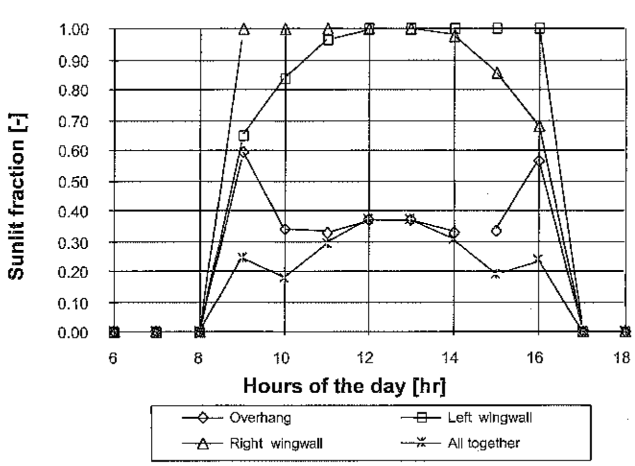


Fig. 5. Sunlit fractions of the window for four shading configurations.

input data and the procedures for calculating under transient conditions, the internal temperature in summer of a single room without any cooling equipment. A validation procedure for the determination of the sunlit area of a window due to external obstructions is included in the proposed standard. The validation procedure requires the evaluation of the sunlit factor, defined as the ratio of the sunlit area of a plane surface to its total area for six defined tests. The sunlit factor used in the CEN [10] standard is equivalent to the sunlit fraction used in this work. The following tests are required by the proposed standard:

- Test 1: South-facing window with an overhang;

Table 1
Sunlit fractions for six tests according to the proposed CEN standard

| Hour | TRNSHD | CEN |
|---|---|---|
| Test 1 | | |
| 7.00 | 0.000 | 0.00 |
| 8.00 | 0.529 | 0.53 |
| 9.00 | 0.238 | 0.24 |
| 10.00 | 0.210 | 0.21 |
| 11.00 | 0.299 | 0.30 |
| 12.00 | 0.327 | 0.33 |
| Test 2 | | |
| 7.00 | 0.000 | 0.00 |
| 8.00 | 0.471 | 0.47 |
| 9.00 | 0.762 | 0.76 |
| 10.00 | 0.967 | 0.97 |
| 11.00 | 1.000 | 1.00 |
| 12.00 | 1.000 | 1.00 |
| Test 3 | | |
| 7.00 | 0.000 | 0.00 |
| 8.00 | 0.000 | 0.00 |
| 9.00 | 0.000 | 0.00 |
| 10.00 | 0.178 | 0.18 |
| 11.00 | 0.299 | 0.30 |
| 12.00 | 0.327 | 0.33 |
| Test 4 | | |
| 7.00 | 0.000 | 0.00 |
| 8.00 | 1.000 | 1.00 |
| 9.00 | 1.000 | 1.00 |
| 10.00 | 1.000 | 1.00 |
| 11.00 | 0.901 | 0.90 |
| 12.00 | 0.847 | 0.84 |
| Test 5 | | |
| 7.00 | 1.000 | 1.00 |
| 8.00 | 0.890 | 0.89 |
| 9.00 | 0.714 | 0.71 |
| 10.00 | 0.391 | 0.39 |
| 11.00 | 0.024 | 0.00 |
| 12.00 | 0.000 | 0.00 |
| Test 6 | | |
| 7.00 | 0.000 | 0.00 |
| 8.00 | 0.000 | 0.00 |
| 9.00 | 0.071 | 0.07 |
| 10.00 | 0.719 | 0.72 |
| 11.00 | 1.000 | 1.00 |
| 12.00 | 1.000 | 1.00 |

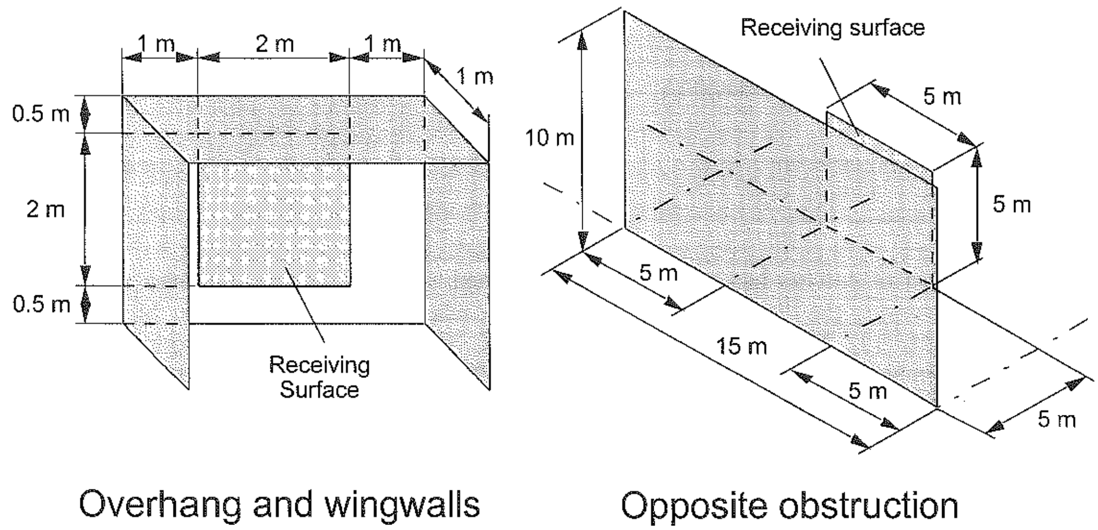


Fig. 6. Dimensions of the window and its obstructions according to the proposed standard.

- Test 2: South-facing window with two wingwalls;
- Test 3: South-facing window with an overhang and two wingwalls;
- Test 4: South-facing window with an opposite obstruction;
- Test 5: East-facing window with an overhang; and
- Test 6: East-facing window with an opposite obstruction.

The dimensions of the window and its obstructions for the six tests are shown Fig. 6. The location of the window is at a latitude of 508° N and a longitude of −158°. The validation procedure requires that for each test instantaneous values of the sunlit factor should be determined on 15 July at each hour, or each half hour from 07:00. to 12:00 h solar time. Due to the resolution of TRNSHD hourly values are used for validation. In order to obtain instantaneous sunlit fractions, the averaging of the hour angle in TRNSHD is turned off.

The results of the calculations with TRNSHD and the reference values given in the proposed standard are shown in Table 1. The validation procedure allows a deviation of 0.05 for each value. It can be seen that good agreement of the results is obtained and that TRNSHD meets the requirements of the proposed CEN standard. In general, the rounded sunlit fractions of TRNSHD are equal to the given values.

## 5. Diffuse radiation shading

For validation, the results of the diffuse radiation shading procedure are compared to those of TRNSYS TYPE 34. TYPE 34 and TRNSHD use different approaches. TYPE 34 calculates the view factor from the receiver surface to the sky by subtracting the view factor from the window to the overhang and wingwalls from the view factor of an unshaded vertical surface to the sky. For determining the view factors from the window to the overhang and wingwalls, TYPE 34 integrates over the receiver area. TRNSHD determines the sunlit fraction of a receiver surface for diffuse radiation by discretizing the sky into patches and a summing over all patches. In order to obtain comparable results, the sunlit fractions of TRNSHD are converted to view factors by multiplication with the view factor of an unshaded window to the sky. Similar to the validation of beam radiation shading calculation, combinations of the basic overhang and wingwall configuration as shown in Fig. 4 are chosen:

- a south-facing window with an overhang;
- a south facing window with a wingwall; and
- a south-facing window with an overhang and two wingwalls.

Also, the diffuse shading calculations with TRNSHD are performed for a different number of patches, because the accuracy depends on the number of patches used in the discretization procedure of the sky. A greater number of patches improves the accuracy, but increases also the computing efforts.

Table 2 presents the resulting view factors of the window to the sky. The results show that an increasing number of patches in TRNSHD improves the accuracy and yields a good agreement with the results of TYPE 34. For 240 and 7200 patches, both programs gave the same first three digits and a deviation of less than 0.1%. However, 72 patches also yields satisfactory results. For a single overhang, a deviation of 0.4% is obtained. A deviation of 1.0% results for a single wingwall. The largest deviation of 2.7% is encountered when all three obstructions are used together.

Table 2
View factors of the window to the sky for different shading configurations

| | TYPE 34 and TRNSYS | TRNSHD, 72 patches | TRNSHD, 240 patches | TRNSHD, 7200 patches |
|---|---|---|---|---|
| One overhang | 0.4455 | 0.4439 | 0.4451 | 0.4452 |
| One wingwall | 0.4782 | 0.4733 | 0.4783 | 0.4781 |
| One overhang and two wingwalls | 0.4018 | 0.3906 | 0.4016 | 0.4013 |

The impact of the number of patches has been investigated in more detail by varying the dimensions of the overhang and the wingwalls [13]. The improvement in accuracy by using 240 patches instead of 72 is small. For 72 patches the largest deviation amounts to 4.2%. In general, a deviation of less than 1% is obtained. The results leads to the conclusion that using 72 patches is appropriate for diffuse radiation shading of buildings.

## 6. Internal solar distribution of beam radiation

The distribution procedure of beam radiation on inside surfaces of a room is validated against experimental measurements and computer simulations by Messadi [11]. Fig. 7 shows the dimensions of the test room used by Messadi. The test room is a rectangle parallelipipedic enclosure with a single, south oriented window. The experimental set-up was located at the University of Michigan–Ann Arbor.

Experiments for two different window sizes and locations on the south-facing wall, case A and case B, were performed. Instantaneous measurements of the sunlit area on the internal surfaces of the room were taken every hour in solar time. For the window configuration A the measurements were recorded on 29 October, for case B the measurements were taken on 24 November. In addition to the measured values, calculated values of the sunlit area of internal surfaces are presented by Messadi. The Messadi program simultaneously tests for angular boundaries that are established for each of the 64 sunlit configurations that can occur in a rectangle, parallelipipedic enclosure with a single, south oriented window. In order to obtain comparable results, the sunlit fractions of TRNSHD must be converted into sunlit areas on the inside surfaces by the following equation:

$$A_{\text{sunlit},\ k} = f_{\text{beam},\ \text{in},\ k} A_{\text{window}} \left| \frac{\cos \alpha_{\text{window}}}{\cos \alpha_k} \right| \tag{6}$$

where $A_{\text{sunlit},k}$ is the sunlit area of the inside surface $k$, $f_{\text{beam,in},k}$ is the sunlit fraction of the inside surface $k$ for beam radiation, $A_{\text{window}}$ is the total area of the window, $\alpha_{\text{window}}$ is the angle between the sun vector and the normal vector of the window and $\alpha_k$ is the angle between the sun vector and the normal vector of the inside surface $k$.

Tables 3 and 4 show the resulting sunlit areas of the internal walls of the test room from the experimental measurements and calculations performed by Messadi and from the calculations performed by TRNSHD. It can be seen that the sunlit areas calculated by Messadi and the sunlit areas calculated by TRNSHD show good agreement. In general, they give the same first two digits. The remaining deviation between the results can be caused by the determination of the declination because the exact latitude used by Messadi is not known. Comparing the measured values with the calculated values of TRNSHD, deviations of up to 0.3 $\text{ft}^2$ are obtained. These deviations can also be caused by errors related to the conditions of the experiment. According to Messadi, the main error source rises from the fact that the boundaries of the sunlit areas are hard to determine due to a lack of sharpness of the line between shadow and light. Also, the measurements were taken manually with a steel graduated ruler and simultaneous measurements of all dimensions of the sunlit configuration could not be achieved, especially when the latter falls over three internal surfaces. A relative error between the measurements and the results of TRNSHD of the total sunlit area of all internal walls is calculated for each hour of the day. For case A, the largest encountered hourly error amounts to 8%, for case B the largest error turned out to be 2%. These hourly errors are acceptable consider-

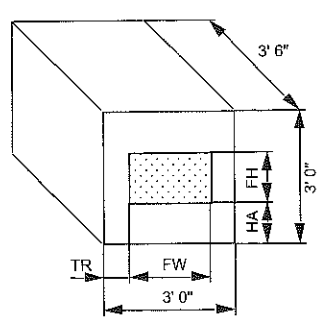


| | Case A | Case B |
|---|---|---|
| Window width FW | 2' 0" | 1' 4" |
| Window height FH | 1' 4" | 2' 0" |
| Distance HA | 10" | 6" |
| Distance TR | 6" | 10" |

Fig. 7. Dimensions of the test room.

Table 3
Sunlit areas [ft$^2$] on the internal surfaces for case A on 29 October[a]

| Hours | Measured | Calculated | TRNSHD |
|---|---|---|---|
| West wall | | | |
| 12.00 | 0.0000 | 0.0000 | 0.0000 |
| 13.00 | 0.0000 | 0.0000 | 0.0000 |
| 14.00 | 0.0000 | 0.0000 | 0.0000 |
| 15.00 | 0.0000 | 0.0000 | 0.0000 |
| 16.00 | 0.0000 | 0.0000 | 0.0000 |
| 17.00 | 0.0000 | 0.0000 | 0.0000 |
| East wall | | | |
| 12.00 | 0.0000 | 0.0000 | 0.0000 |
| 13.00 | 0.9431 | 0.9535 | 0.9553 |
| 14.00 | 2.0496 | 2.3524 | 2.2468 |
| 15.00 | 2.4671 | 2.3429 | 2.3419 |
| 16.00 | 1.6944 | 1.6176 | 1.6156 |
| 17.00 | N/A | 1.0036 | 1.0014 |
| Ground wall | | | |
| 12.00 | 4.0416 | 4.0251 | 4.0266 |
| 13.00 | 3.4459 | 3.6470 | 3.6470 |
| 14.00 | 1.8281 | 1.8569 | 1.9680 |
| 15.00 | 0.3131 | 0.3251 | 0.3230 |
| 16.00 | 0.0000 | 0.0000 | 0.0000 |
| 17.00 | 0.0000 | 0.0000 | 0.0000 |
| North wall | | | |
| 12.00 | 0.0000 | 0.0000 | 0.0000 |
| 13.00 | 0.0000 | 0.0000 | 0.0000 |
| 14.00 | 0.0055 | 0.0065 | 0.0066 |
| 15.00 | 0.0000 | 0.0000 | 0.0000 |
| 16.00 | 0.0000 | 0.0000 | 0.0000 |
| 17.00 | 0.0000 | 0.0000 | 0.0000 |

[a] Measured and calculated values according to Messadi [11].

ing the errors related to the conditions of the experiment. Also, the results show that the sunlit areas appropriately appeared at the expected location on the internal surfaces of the room.

## 7. Shading study with TRNSHD

A more complex shading case study is performed in order to demonstrate the capabilities of the program. In addition, the use of TRNSHD for other objects than buildings is discussed.

## 8. Shading study of an atrium

For the case study, a building with an atrium is chosen as shown in Fig. 8. Atria and sunspaces have become a major architectural component of a building design and a challenge for energy engineering. In general, atria posses large external glazing surfaces. The judicious admission of sunlight into an atrium creates its high aesthetic values. Besides the ambience of an atrium provided by the admission of sunlight, the large glazing surfaces can contribute to high cooling and heating loads. The design of an atrium with respect to both aesthetic values and energy efficiency is a very complex task and requires a detailed shading study and thermal analysis of the atrium.

The building with atrium used in the following shading study is an L-shaped building with three stories as shown in Fig. 8. The atrium has a southeast facing vertical glass wall and a sloped glass roof. The building has two neighbor buildings where one is located to the south and the other one to the east. The neighbor buildings are modeled as "boxes" with the same height as the investigated building. The building is located in Madison, WI at a longitude of 89.48° and a latitude of 43.18°N. For radiation data, a TMY weather data file

Table 4
Sunlit areas [ft$^2$] on the internal surfaces for case B on 24 November[a]

| Hours | Measured | Calculated | TRNSHD |
|---|---|---|---|
| East wall | | | |
| 8.00 | 0.0000 | 0.0000 | 0.0000 |
| 9.00 | 0.0000 | 0.0000 | 0.0000 |
| 10.00 | 0.0000 | 0.0000 | 0.0000 |
| 11.00 | 0.0000 | 0.0000 | 0.0000 |
| 12.00 | 0.0000 | 0.0000 | 0.0000 |
| 13.00 | 0.6451 | 0.4468 | 0.4489 |
| 14.00 | 2.8663 | 2.8788 | 2.8829 |
| 15.00 | 2.6132 | 2.7158 | 2.7157 |
| 16.00 | N/A | 1.9084 | 1.9067 |
| West wall | | | |
| 8.00 | N/A | 1.9083 | 1.9067 |
| 9.00 | N/A | 2.7158 | 2.7157 |
| 10.00 | 2.5907 | 2.8788 | 2.8829 |
| 11.00 | 0.3881 | 0.4471 | 0.4489 |
| 12.00 | 0.0000 | 0.0000 | 0.0000 |
| 13.00 | 0.0000 | 0.0000 | 0.0000 |
| 14.00 | 0.0000 | 0.0000 | 0.0000 |
| 15.00 | 0.0000 | 0.0000 | 0.0000 |
| 16.00 | 0.0000 | 0.0000 | 0.0000 |
| Ground wall | | | |
| 8.00 | 0.0000 | 0.0000 | 0.0000 |
| 9.00 | N/A | 0.3843 | 0.3811 |
| 10.00 | 2.1994 | 1.9471 | 1.9438 |
| 11.00 | 3.4188 | 3.2798 | 3.2780 |
| 12.00 | 3.4444 | 3.3532 | 3.3512 |
| 13.00 | 3.1909 | 3.2798 | 3.2780 |
| 14.00 | 1.9705 | 1.9471 | 1.9438 |
| 15.00 | 0.4792 | 0.3843 | 0.3811 |
| 16.00 | 0.0000 | 0.0000 | 0.0000 |
| North wall | | | |
| 8.00 | 0.0000 | 0.0000 | 0.0000 |
| 9.00 | 0.0000 | 0.0000 | 0.0000 |
| 10.00 | 0.1388 | 0.1358 | 0.1353 |
| 11.00 | 0.8333 | 0.9259 | 0.9279 |
| 12.00 | 0.8055 | 0.9647 | 0.9672 |
| 13.00 | 0.9062 | 0.9261 | 0.9279 |
| 14.00 | 0.1279 | 0.1358 | 0.1353 |
| 15.00 | 0.0000 | 0.0000 | 0.0000 |
| 16.00 | 0.0000 | 0.0000 | 0.0000 |

[a] Measured and calculated values according to Messadi [11].

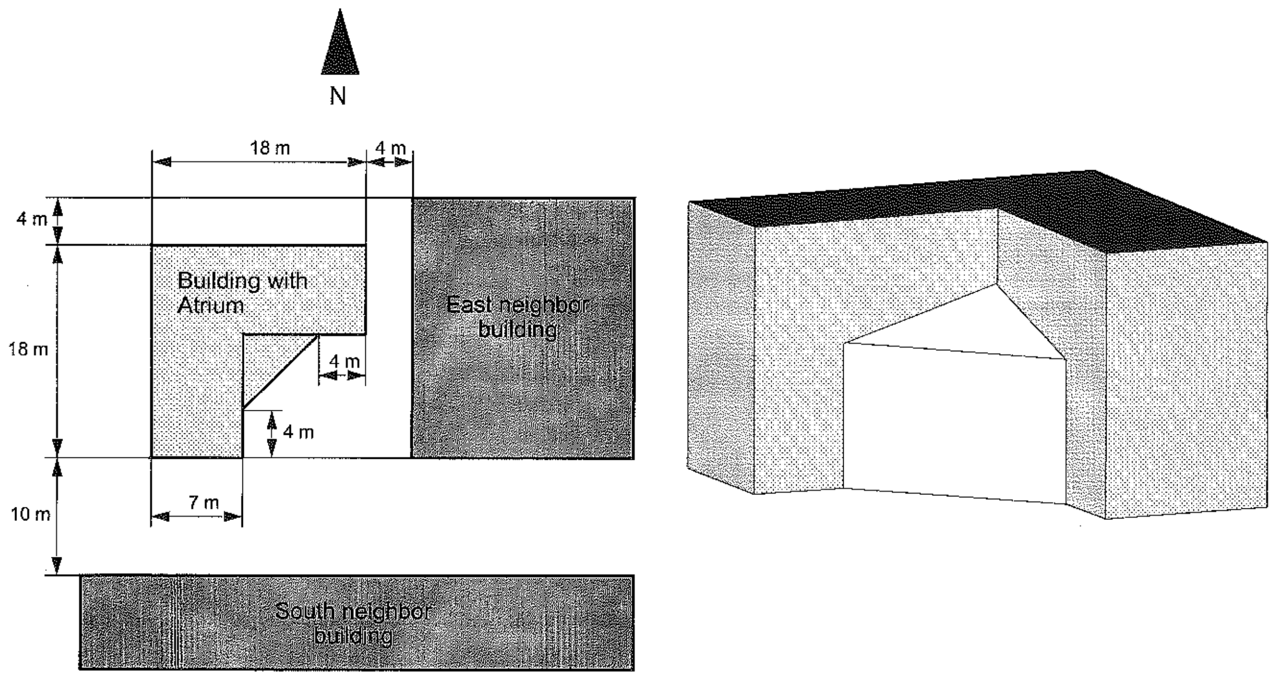


Fig. 8. Building with atrium and surroundings.

from Madison is used. Shading can occur from the building itself and the neighbor buildings. For the shading study of the atrium three levels of shading calculations are chosen:

- case 1: no external shading;
- case 2: shading originated by the building itself; and
- case 3: shading originated by the building itself and its neighbor buildings.

The shading calculations of beam and diffuse radiation are performed with TRNSHD. In order to examine the impact of the shading on the amount of solar radiation incident on a surface, the resulting sunlit fraction of the calculations with TRNSHD are used in monthly simulations with TRNSYS. The solar radiation incident on a surface is calculated by:

$$\bar{G} = G_{\text{unshaded}} f \tag{7}$$

where $\bar{G}$ is the average irradiance level over the whole receiver surface, $G_{\text{unshaded}}$ is the irradiance level of the unshaded receiver surface and $f$ is the sunlit fraction.

Figs. 9 and 10 show the resulting monthly radiation on the vertical glass wall and the glass roof of the atrium. It can be seen that for the glass wall the impact of the neighbor buildings is large compared to the impact of the selfshading of the building, whereas for the glass roof the impact of the selfshading of the building is more important. The Figures also show that for this atrium the diffuse radiation contributes a

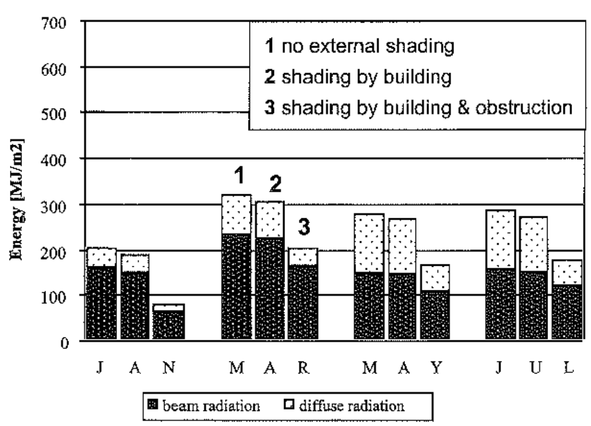


Fig. 9. Monthly radiation on the glass wall for the three shading configurations.

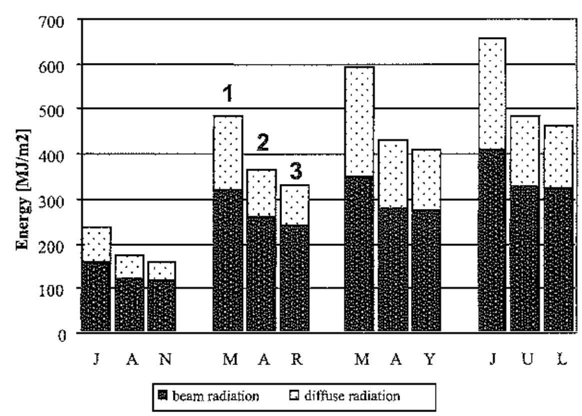


Fig. 10. Monthly radiation on the glass roof for the three shading configurations.

significant portion of the total monthly radiation. Thus, neglecting diffuse radiation shading yields an overprediction of solar gains for the investigated atrium. Fig. 11 illustrates the diffuse shading effect in more detail. In Fig. 11, the patches of the hemisphere are shown in two dimensions and each patch is colored according to the corresponding sunlit fraction. In addition to the sunlit fraction for each patch, the resulting sunlit diffuse fraction for the atrium surfaces is shown in Fig. 11. For the vertical glass wall of the atrium, the blocking of diffuse sky radiation by the building itself is small; 95% of the diffuse radiation still strikes the wall. The impact of the neighbor buildings is relative high. If the neighbor buildings are also considered, then the diffuse radiation access is reduced to 44% compared to an completely unshaded wall. The results illustrate how important it is to consider not only the building in question, but also its surroundings. For the glass roof, the impact of diffuse sky radiation is reduced to 65% by shading through the building itself. Neighbor buildings cause a further reduction of the diffuse radiation down to 57%.

A generalization of the results and conclusions obtained for the one individual atrium is not valid, because the results depend strongly on the weather data, the location and geometric configuration.

## 9. Shading study of other objects than buildings

Although TRNSHD was developed for building simulations with TRNSYS, it is a stand-alone tool that can used for problems other than buildings. In general, every type of solar receiver, like a thermal flat-plate collector or a photovoltaic panel that can be approximated by planar polygons, can be handled by

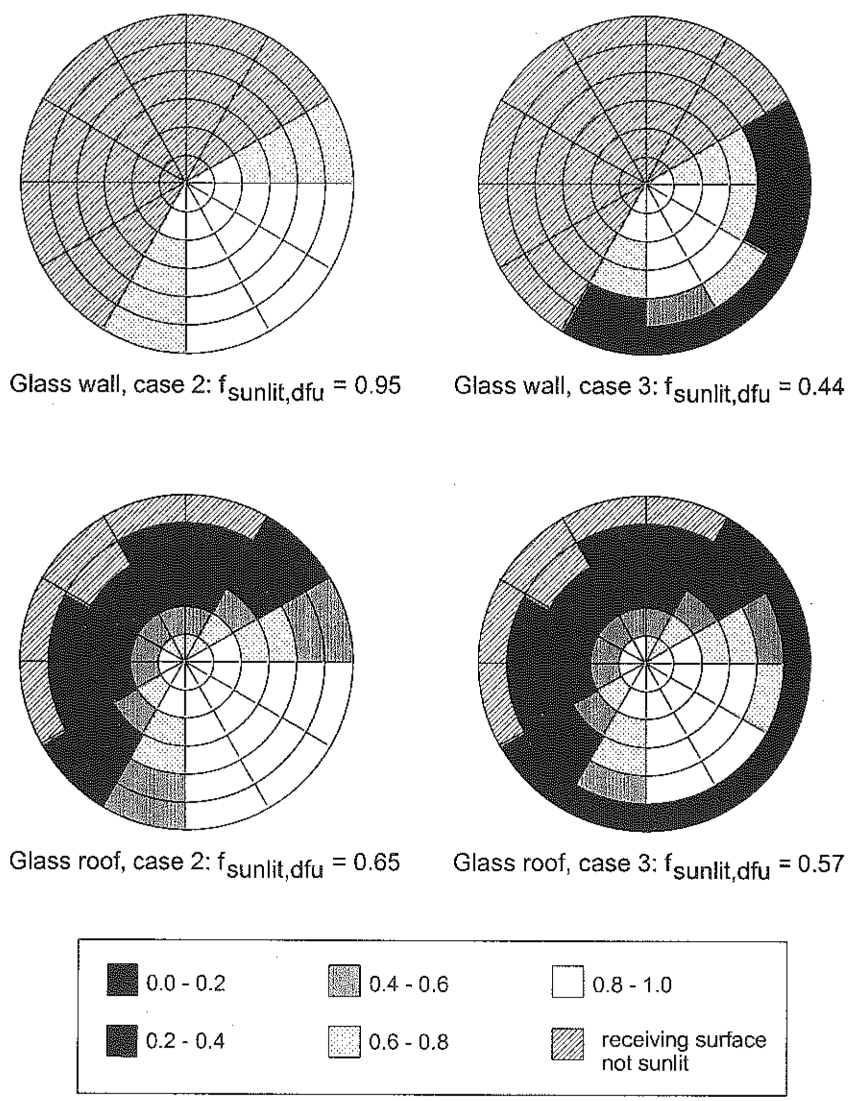


Fig. 11. Diffuse sunlit fractions for atrium glazing.

TRNSHD. However, it needs to be assured that an average radiation level over the whole receiver area is an appropriate approach. For solar collectors it is usually adequate to use an average radiation level [12], but for photovoltaic systems the effect on power by using average radiation may not be correct.

## 10. Conclusions

A computer program for external shading and internal insolation calculations of solar beam and diffuse radiation has been developed. The calculation techniques has been implemented in a software application called TRNSHD. TRNSHD is a stand-alone tool, which has been developed for building simulations with TRNSYS. However, TRNSHD is not restricted to buildings or TRNSYS.

The program TRNSHD has been validated against other computer programs (including ASHRAE algorithm), a proposed European Standard and measurements. The validation process shows that TRNSHD functions correctly and the results of TRNSHD are in good agreement with expected values. Also, it shows that the sunlit areas appropriately appeared at the expected location. In the validation process, it has been found that a total number of 72 sky patches yields an acceptable accuracy when calculating diffuse radiation shading. A discussion of the frequency at which beam radiation is performed yields the conclusion that calculations on an average day of each month is sufficient.

Finally, a complex shading case study of building with an atrium has demonstrated the use and the capabilities of TRNSHD. The study illustrated that the surroundings of a building, like neighbor buildings and the landscape, can have a significant impact on the amount of solar radiation that strikes an external surface. However, the generalization of results of shading calculations is difficult, because they depend strongly on the location, the weather data and the geometry.

## Acknowledgements

This research was made possible by contributions from TRANSSOLAR Energietechnik GmbH, Stuttgart and the Solar Energy Laboratory of the University Wisconsin–Madison. The author gratefully acknowledge their support of this project.

## References

[1] EREN. Energy efficiency and renewable energy network. US Department of Energy, http:/www.eren.doe.gov/, 1996.
[2] Klein SA. Calculation of monthly average insolation on tilted surfaces. Solar Energy 1977;19:325.
[3] SEL. TRNSYS manual version 14.1. Madison: Solar Energy Laboratory, University of Wisconsin, 1995.
[4] Winkelmann FC. Personal communication. Lawrence Berkeley National Laboratory, 1996.
[5] Walton GN. The application of homogeneous coordinates to shadowing calculations. ASHRAE Trans 1979;85(1):174–80.
[6] Weiler K, Atherton P. Hidden surface removal using polygon area sorting. Computer Graphics 1977;11:214–22.
[7] O'Rourke J. Computational geometry in C. Cambridge University Press, 1994.
[8] Johnston SA. Solar test (SOLTST): subroutine to solar graphics. Master thesis, School of Architecture and Urban Planning. University of Wisconsin–Milwaukee, 1985.
[9] ASHRAE. Subroutine algorithms for heating and cooling loads to determine building energy requirements. Compiled by subcommittee for heating and cooling loads. ASHRAE Task Group on Energy Requirements, 1975.
[10] CEN. Thermal performance of buildings — internal temperatures in summer of a room without mechanical cooling — general criteria and calculation procedures. CEN TC89. European Committee for Standardization, Brussels, 1995.
[11] Messadi MT. Experimental validation of the procedure to determine the internal sunlit configurations. In: Proceedings of the 15th National Passive Solar Conference. American Solar Energy Society, 1990. p. 251–6.
[12] Duffie JA, Beckman WA. Solar engineering of thermal processes. 2nd ed. Wiley and Sons, 1991.
[13] Hiller, MDE. TRNSHD — A program for shading and insolation calculations. Master thesis, Mechanical Engineering Department. University of Wisconsin–Madison, 1996.